Theoretical considerations of transition to turbulence in natural convection near a vertical wall

A. Bejan and G. R. Cunnington*

Hydrodynamic stability analysis of an inviscid wall jet shows that instability is possible above a characteristic disturbance wavelength which is proportional to the jet thickness. This scaling is the basis for an argument that transition occurs when the fluctuating time period of the unstable (inviscid) wall jet is of the same order as the viscous diffusion time normal to the jet. The transition must occur when the jet Reynolds number is of the order of 10^2. Published observations of transition along a heated vertical wall are reviewed in order to test the validity of the proposed scaling argument. Specifically, numerous observations on buoyant jets near isothermal walls, near constant-heat-flux walls, and in enclosures with vertical isothermal walls are shown to support the validity of the transition mechanism proposed

Key words: *convection, turbulence, fluid flow*

Transition phenomena have been studied extensively during the past half-century. This work has been brought in perspective in a number of review papers, for example by Tani[1] and Reshotko[2] for boundary layer flow and by Gebhart[3] for natural convection flow.

The object of this study is to propose a scaling argument as basis for transition to turbulence in the wall jet flows encountered in natural convection along heated vertical walls. First, linear stability analysis of a wall jet indicates that the flow is unstable to disturbance wavelengths greater than a certain multiple of the jet thickness D. Based on this proportionality, it will be argued that transition is ruled by the internal competition between two time scales, the jet fluctuation period and the time of viscous penetration normal to the flow direction. A comprehensive review of the published experimental observations on transition supports the validity of this scaling argument. Finally, it is shown that photographs and numerical simulations of transition in vertical enclosures heated from the side visualise the transition mechanism described.

Hydrodynamic instability of an inviscid wall jet

Consider the flow of an inviscid jet $U(y)$ next to a vertical wall, as shown in Fig 1. We want to know the waviness of the jet as it becomes unstable, in other words, the frequency of its fluctuation relative to a fixed spot on the wall, which can be obtained by performing a linearised stability analysis of the flow. This analytical approach is outlined by Lamb[4]. By superimposing on the base flow ($u = U$, $v = 0$) unspecified disturbances:

$$u = U + u' \tag{1}$$

$$v = v' \tag{2}$$

the inviscid flow (Euler) equations yield the vorticity transport equation:

$$\frac{\partial \tau}{\partial t} + (U + u')\frac{\partial \tau}{\partial x} + v'\frac{\partial \tau}{\partial y} = 0 \tag{3}$$

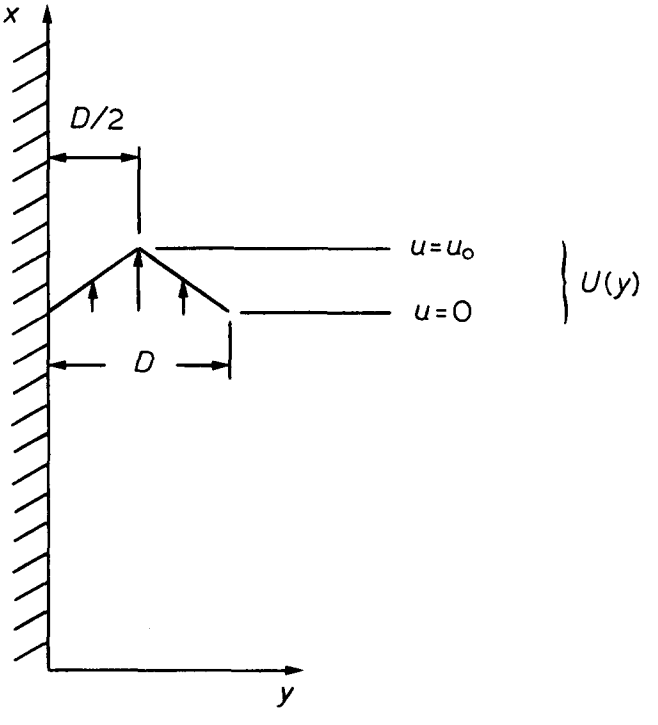

Fig 1 Wall jet velocity profile

* Department of Mechanical Engineering, University of Colorado, Box 427, Boulder, Colorado 80309, USA
Received 9 August 1982 and accepted for publication on 12 April 1983

 0142-727X/83/030131-09$03.00

with the vorticity defined as:

$$\tau = \frac{\partial v'}{\partial x} - \frac{\partial u'}{\partial y} - \frac{dU}{dy} \tag{4}$$

Linearising Eq (3) yields:

$$\left(\frac{\partial}{\partial t} + U\frac{\partial}{\partial x}\right)\left(\frac{\partial v'}{\partial x} - \frac{\partial u'}{\partial y}\right) - \frac{d^2U}{dy^2}v' = 0 \tag{5}$$

Next assume that the disturbance velocity components are both periodic in x:

$$u' = u_* e^{i(kx+\sigma t)} \tag{6}$$

$$v' = v_* e^{i(kx+\sigma t)} \tag{7}$$

where k is the wavenumber ($k = 2\pi/\lambda$). Substitution of Eqs (6, 7) into the vorticity transport equation and the mass continuity equation, and the elimination of u_* yields a single equation for the transversal disturbance amplitude v_*,

$$(\sigma + kU)\left(\frac{\partial^2 v_*}{\partial y^2} - k^2 v_*\right) - \frac{d^2U}{dy^2}kv_* = 0 \tag{8}$$

Our interest is in the wavelengths λ or wavenumbers k for which σ is imaginary, ie for which the assumed disturbance is likely to be amplified (Eqs 6, 7). As shown in Fig 1, we assume a triangular velocity profile, so that in all regions of the flow $d^2U/dy^2 = 0$:

$$\text{I)} \quad U = \frac{u_0}{D/2}y, \qquad 0 < y < D/2$$

$$\text{II)} \quad U = \frac{u_0}{D/2}(D - y), \qquad D/2 < y < D \tag{9}$$

$$\text{III)} \quad U = 0, \qquad D < y$$

Solving Eq (8), the corresponding expressions for v_* in the three regions are:

$$\text{I)} \quad v_* = A e^{-ky} + B e^{ky}$$

$$\text{II)} \quad v_* = C e^{-ky} + D_0 e^{ky} \tag{10}$$

$$\text{III)} \quad v_* = E e^{-ky} + F e^{ky}$$

The solid wall condition, $v_* = 0$ at $y = 0$, and the condition that v_* must be finite infinitely far from the wall, mean that:

$$A + B = 0 \tag{11}$$

$$F = 0 \tag{12}$$

Two more equations follow the condition that v_* must vary continuously from region I to II, and from II to III:

$$A e^{-kD/2} + B e^{kD/2} = C e^{-kD/2} + D_0 e^{kD/2} \tag{13}$$

$$C e^{-kD} + D_0 e^{kD} = E e^{-kD} \tag{14}$$

Finally, the condition that the pressure must vary continuously from one region to the next amounts to integrating Eq (8) across one region-to-region interface (eg from $y = D^-$ to $y = D^+$)[4]:

$$(\sigma + kU)\left[\left(\frac{\partial v_*}{\partial y}\right)_+ - \left(\frac{\partial v_*}{\partial y}\right)_-\right] - kv_*\left[\left(\frac{dU}{dy}\right)_+ - \left(\frac{dU}{dy}\right)_-\right] = 0 \tag{15}$$

Notation

A, B, C, D_0, E, F	Coefficients (Eq 10)
D	Jet thickness
g	Gravitational acceleration (in negative x direction)
G^*	$5^{4/5}\left(g\frac{\beta H^4}{k\nu^2}\right)$ (Eq 49)
H	Vertical length scale
k	Wavenumber ($2\pi/\lambda$)
L	Horizontal dimension of enclosure
m	$\sigma D/u_0 + 1$ (Eq 18)
N_B	t_v/t_{min} (Eq 29)
Pr	Prandtl number
Ra	Rayleigh number: Ra_H—based on vertical length scale H; Ra_L—based on cavity width L
Re	Reynolds number
S	vertical temperature gradient
t	Time
T	Temperature
u	Velocity parallel to the wall (x-direction)
v	Velocity normal to the wall (y-direction)
$u_* v_*$	Disturbance amplitudes
α_c	Critical wavenumber ($2\pi L/\lambda_c$)
α	Thermal diffusivity
β	Coefficient of thermal expansion
γ	$e^{-kD/2}$ (Eq 18)
γ	Dimensionless stratification parameter $\left(\frac{1}{4}S\frac{L}{\Delta T}Ra_L\right)^{1/4}$
δ_T	Thermal boundary layer thickness
δ_V	Boundary layer where vertical velocity obeys a no-slip condition
λ	Wavelength
τ	Vorticity
σ	Disturbance growth rate
ν	Kinematic viscosity

Subscripts and superscripts

*	Uniform heat flux
'	Disturbances
min	Minimum
v	Viscous
B	Buckling [6,8,32]

Applying this condition twice, at $y=D/2$ and at $y=D$, yields two more equations:

$$D_0\left(\frac{\sigma D}{u_0}+1\right)e^{kD/2}+Ce^{-kD/2}=0 \tag{16}$$

$$\left[1-\frac{D}{4u_0}(\sigma+ku_0)\right]C+\left[1+\frac{D}{4u_0}(\sigma+ku_0)\right]D_0 +\frac{D}{4u_0}(\sigma+ku_0)(A-B)=0 \tag{17}$$

Eqs (11, 13, 14, 16, 17) are all homogeneous and, together, they constitute a system for determining the five unknown coefficients A, B, C, D_0, E. A non-trivial solution is possible if the determinant of this system is zero:

$$m^2+m(2\gamma^2+kD-3-\gamma^4)-\gamma^4(1+kD)+2\gamma^2=0 \tag{18}$$

where $\gamma=e^{-kD/2}$ and $m=\sigma D/u_0+1$. Eq (18) is obtained by systematically eliminating the five coefficients among Eqs (11, 13, 14, 16, 17). Whether or not σ is imaginary depends on the character of m: since Eq (18) is a quadratic in m, am^2+bm+c, imaginary roots are possible if the discriminant $\Delta=b^2-4ac$ is negative, ie when:

$$\Delta=(2\gamma^2+kD-3-\gamma^4)^2+4\gamma^4(1+kD)-8\gamma^2<0 \tag{19}$$

Solving $\Delta=0$ we find that the wall jet of Fig 1 is unstable ($\Delta<0$) if

$$1.337<kD<3.427 \tag{20}$$

In other words, the inviscid wall jet is likely to acquire a waviness described by wavelengths in the range

$$1.833<\frac{\lambda}{D}<4.701 \tag{21}$$

The conclusion that an inviscid wall jet of thickness D is unstable only in a certain range of disturbance wavelengths, agrees with earlier results concerning other inviscid flows. For example, Rayleigh[5] found that a free two-dimensional jet of triangular profile is unstable for wavelengths $\lambda>1.714D$. Rayleigh also found[5] that a free shear layer of thickness D is unstable if $\lambda>4.914D$. It is significant that for several different base flows, from the wall jet of Fig 1 to Rayleigh's free shear layer, the edges of the wavelength domains for inviscid instability are marked by wavelengths which scale with the flow thickness D. We feel that this scaling is important and, ultimately, responsible for the phenomenon of transition to turbulence[6]. This scaling is the basis for the transition criterion outlined next.

Time scale criterion for transition

Each longitudinal length scale λ and the jet velocity U define a time scale:

$$t\sim\frac{\lambda}{U/2} \tag{22}$$

This time scale is the period of the jet fluctuation as seen by an observer positioned on the vertical wall. Note that $U/2$ is, in an order of magnitude sense, the wave velocity relative to a fixed spot on the wall.

Thus, the fluctuation time of the wall jet as an inviscid stream is:

$$t\geqslant t_{\min}=\frac{\lambda_{\min}}{U/2} \tag{23}$$

where, according to Eq (21):

$$\lambda_{\min}=1.833D \tag{24}$$

In conclusion, $t_{\min}\sim D$; this proportionality appears as a straight line in Fig 2, showing that an inviscid wall jet of thickness D can become unstable within a time interval $t>t_{\min}$.

The issue of whether or not the wall jet will become unstable is decided by examining the 'inviscidity' of the flow. Inviscidity or viscidity is a flow property, not a fluid property. If the wall jet tends to fluctuate (wave), then jet fluid will tend to make contact with the solid wall and the adjacent semi-infinite fluid reservoir intermittently, at time intervals $t>t_{\min}$. The wall jet, as a flow, remains inviscid if during each interval t it cannot learn by viscous diffusion of the presence of a restraining ambient. The characteristic time of viscous penetration (t_v) from the wall and from the outer edge of the jet to the jet centreline (over a distance $D/2$) is given by the solution to Stokes' first problem[7]:

$$\frac{D/2}{2\sqrt{\nu t_v}}\sim 1 \tag{25}$$

or:

$$t_v\sim\frac{D^2}{16\nu} \tag{26}$$

Locally, no jet will remain inviscid forever. Fig 2 shows that if the fluctuation time exceeds the viscous

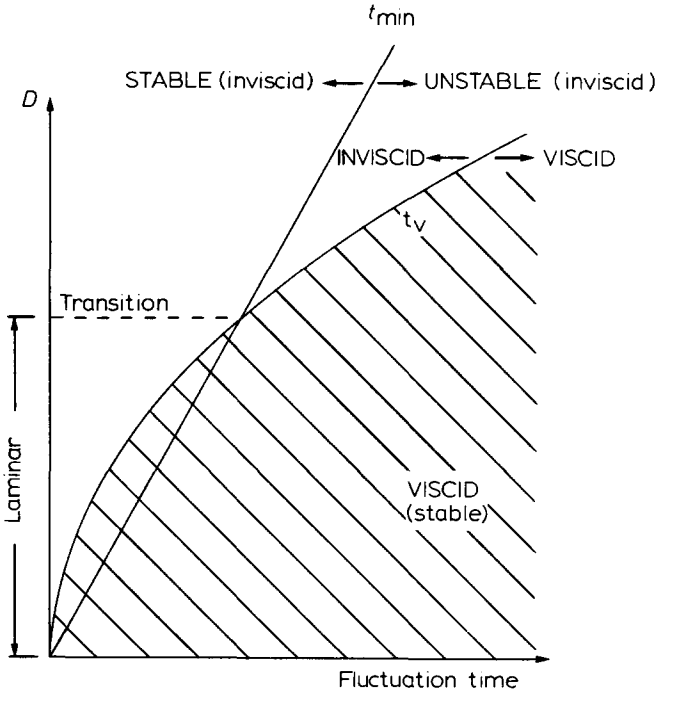

Fig 2 Internal competition between two characteristic times, the minimum period for inviscid instability (t_{min}) and the viscous communication time[6] (t_v)

communication time t_v, the jet will remain laminar because it will continue to be restrained viscously by its ambient.

The instability predicted by so many hydrodynamic stability studies is therefore possible only if t_v exceeds t_{min}. In Fig 2, this condition corresponds to the intersection of the $t_{min} \sim D$ line with the $t_v \sim D^2$ line:

$$t_{min} = t_v \tag{27}$$

The phenomenon of transition to non-laminar flow appears to be governed by the time criterion:

$$O(N_B) = 1 \tag{28}$$

where:

$$N_B = \frac{t_v}{t_{min}} = \frac{DU}{58\nu} \tag{29}$$

The object of the remaining presentation is to test the $N_B \sim 1$ criterion against the voluminous experimental record available on transition in natural convection along a vertical heated wall. Note at this point that the $N_B \sim 1$ criterion is equivalent to $Re \sim 58 \gg 1$, where the Reynolds number Re is based on the local U, D scales of the buoyant wall jet. Experimentally (as described later) it is found that the transition corresponds to a Re constant considerably greater than unity ($Re \sim 10^2$). The contribution of the time scale argument that led to Eq (29) is to predict a transition Re much greater than unity; unlike the present arguments, classical scaling arguments regarding the relative size of viscous and inertial terms in the Navier–Stokes equations or in the Orr–Sommerfeld equation reveal $Re \sim 1$ as a critical dimensionless parameter.

It is also worth noting that, theoretically, the same transition criterion ($N_B \sim 1$, or $Re \sim 10^2$) is recommended by the buckling (meandering) property of inviscid streams[8]. This coincidence arises because the buckling wavelength of a two-dimensional inviscid jet[8], $\lambda_B = \pi\sqrt{3}D = 1.81D$, is practically the same as the minimum wavelength for inviscid instability, $\lambda_{min} = 1.83D$. It has been shown[8] that the $N_B \sim 1$ criterion anticipates correctly the transition to turbulence in free jet and wake flow.

Scale analysis of natural convection along a vertical heated wall

To be able to apply the time-scale criterion, a theoretical understanding of the two wall jet scales (U, D) is essential. Consider the flow near a vertical wall, driven by the temperature difference ΔT between wall and fluid reservoir. In general, the flow thickness (D) will differ from the thickness of the fluid layer heated by the wall[9] (δ_T). The boundary layer-approximated equations governing the conservation of mass, momentum and energy in the system shown in Fig 3 are[10]:

$$\frac{\partial u}{\partial x} + \frac{\partial v}{\partial y} = 0 \tag{30}$$

$$u\frac{\partial u}{\partial x} + v\frac{\partial u}{\partial y} = \nu\frac{\partial^2 u}{\partial y^2} + g\beta(T - T_\infty) \tag{31}$$

$$u\frac{\partial T}{\partial x} + v\frac{\partial T}{\partial y} = \alpha\frac{\partial^2 T}{\partial y^2} \tag{32}$$

where x, y, u, v, T, ν, g, β and α are the co-ordinates, velocity components, temperature, kinematic viscosity, gravitational acceleration in the negative x direction, coefficient of thermal expansion and thermal diffusivity, respectively.

Let δ_T be the thermal boundary layer thickness, ie the slender fluid region in which the wall heating effect is felt. In this region, the heat conducted horizontally from the wall into the fluid, represented by the scale $\alpha\Delta T/\delta_T^2$ from the energy equation (Eq (32)), is converted into enthalpy flow in the vertical direction, $u\Delta T/H$. Thus, the balance between conduction and convection in the layer of thickness δ_T requires the following equivalence between the corresponding scales:

$$\frac{u\Delta T}{H} \sim \alpha\frac{\Delta T}{\delta_T^2} \tag{33}$$

or:

$$u \sim \alpha H/\delta_T^2 \tag{34}$$

The momentum equation (31) accounts for the competition between three forces: inertia, friction and buoyancy. The scales of these forces are, in order:

$$\frac{u^2}{H}, \quad \nu\frac{u}{\delta_T^2}, \quad g\beta\,\Delta T \tag{35}$$

Assuming first that the effect of inertia is negligible, and that Eq (31) is a balance between buoyancy and friction, we write:

$$\nu\frac{u}{\delta_T^2} \sim g\beta\,\Delta T \tag{36}$$

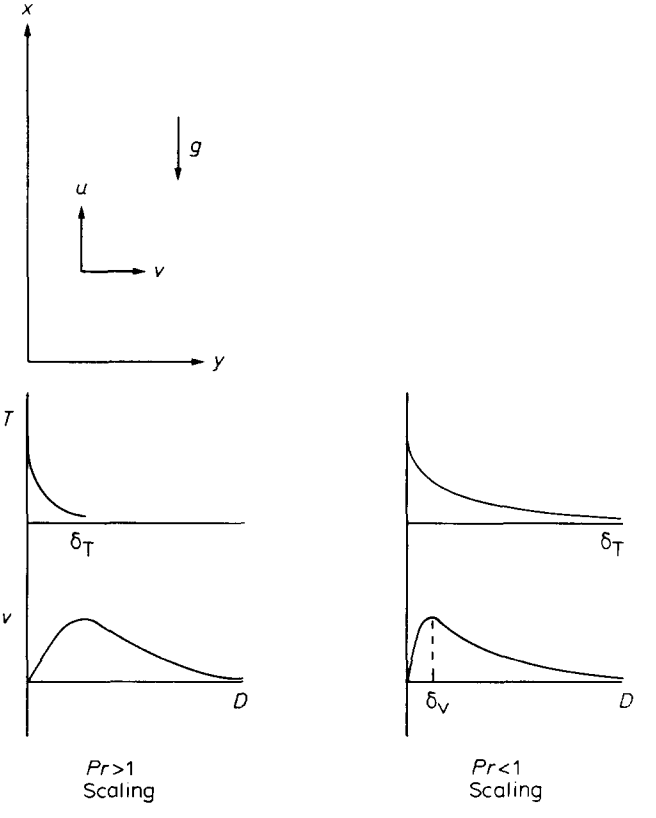

Fig 3 Relative sizes of thermal and velocity boundary layers for high and low Pr *fluids*

Using Eq (34) we find that, in a δ_T layer dominated by a balance between buoyancy and friction, the scales are:

$$\delta_T \sim H Ra_H^{-1/4}$$
$$u \sim \alpha Ra_H^{1/2}/H \quad (37)$$

The Rayleigh number based on vertical length scale H, Ra_H, is defined as

$$Ra_H = \frac{g\beta\,\Delta T H^3}{\alpha\nu} \quad (38)$$

With the same assumptions that led to the scales above (Eq (37)), the negligibly small ratio inertia/friction, or inertia/buoyancy, requires

$$\frac{u^2/H}{u/\delta_T^2} \sim \frac{1}{Pr} \ll 1 \quad (39)$$

In conclusion, the scales are valid in high Prandtl number fluids ($\nu/\alpha \gg 1$): as shown on the left side of Fig 3, $Pr \gg 1$ fluids develop an additional length scale D, which is the thickness of the wall jet referred to in the time criterion for transition (Eqs (28, 29)). The D scale follows from the momentum equation scales (Eq (35)). Outside the thermal boundary layer the fluid is isothermal, hence, the buoyancy force is negligible relative to both inertia and friction. The equivalence of inertia and friction scales in the layer of thickness D:

$$\frac{u^2}{H} \sim \nu\frac{u}{D^2} \quad (40)$$

in conjunction with scales (37) yields:

$$D \sim Pr^{1/2}\delta_T \sim HPr^{1/2}\,Ra_H^{-1/4} \quad (41)$$

for $Pr \gg 1$. The size of the wall jet relative to the thermal boundary layer is shown schematically in Fig 3. The D scale (Eq (41)), will be used later in the application of the transition criterion.

It remains to establish the u, δ_T and D scales prevailing in the case where the momentum equation represents a balance between buoyancy and inertia in the layer of thickness δ_T (note that the $Pr \gg 1$ scales (37) and (41) are based on a friction ~ buoyancy balance in the δ_T layer). Writing:

$$\frac{u^2}{H} \sim g\beta\,\Delta T \quad (42)$$

and using Eq (34) yields:

$$\delta_T \sim H(Ra_H\,Pr)^{-1/4}$$
$$u \sim \alpha(Ra_H\,Pr)^{1/2}/H \quad (43)$$

The inertia ~ buoyancy balance governs the δ_T layer, except in a layer δ_v immediately adjacent to the wall where the vertical velocity v obeys the no-slip condition. In the δ_v layer friction is an important effect, hence:

$$\nu\frac{u}{\delta_v^2} \sim g\beta\,\Delta T \quad (44)$$

Combining this result with the u scale given by Eq (43) yields:

$$\delta_v \sim HRa_H^{-1/4}\,Pr^{1/4} \sim \delta_T\,Pr^{1/2} \quad (45)$$

The relative magnitude of the δ_T and δ_v scales is shown in the right half of Fig 3. Thus, we draw two important conclusions: that the flow scales (43, 45) which follow from a balance between inertia and buoyancy in the δ_T layer correspond to low Prandtl number fluids; and that the thickness of the wall jet in this case is the thickness of the entire layer heated by the wall,

$$D \sim \delta_T \sim H(Ra_H\,Pr)^{-1/4} \quad (46)$$

for $Pr \ll 1$. In what follows we shall rely on the above dimensions to translate the time-scale criterion (28, 29) into the terminology in which the phenomenon of transition has been recorded by previous studies of natural convection.

Transition along a vertical heated wall

A relatively wide selection of experimental observations on the beginning of transition along an isothermal wall was compiled already by Mahajan and Gebhart[11]. Table 1 reproduces this compilation and shows the number G above which the buoyant wall jet was noticed to become nonlaminar. The number G is defined as:

$$G = 4^{3/4}\left(\frac{g\beta\,\Delta T H^3}{\nu^2}\right)^{1/4}$$

in other words:

$$G = 4^{3/4}\,Ra_H^{1/4}\,Pr^{-1/4} \quad (47)$$

The time criterion (28, 29) can be rewritten in terms of G, by using scales (37, 41) for $Pr > 1$ fluids; taking $U \sim u$ we have:

$$N_B = \frac{DU}{58\nu} \sim \frac{1}{58}\,Ra_H^{1/4}\,Pr^{-1/2} \sim \frac{G}{164Pr^{1/4}} \quad (48)$$

Table 1 shows the N_B value corresponding to each experimental report: in all cases $O(N_B) = 1$, which is the same as the time criterion for transition. In conclusion, the experimental data on transition along isothermal walls supports the theoretical argument that the transition phenomenon is marked by the equivalence of time scales $t_{min} \sim t_v$.

Table 2 is a compilation of transition observations made using a vertical wall with constant heat

Table 1 Experimental observations on beginning of transition along a vertical isothermal wall

	Pr	G	N_B
Warner and Arpaci[12]	0.72	466	3.08
Colak-Antic[13]	0.72	572	3.79
Cheesewright[14]	0.72	600	3.97
Regnier and Kaplan[15]	0.72	622	4.12
	0.77	460–547	2.99–3.56
	0.77	645–702	4.20–4.57
	0.77	541	3.52
	0.77	605	3.94
	0.77	378	2.46
Eckert and Soehngen[16]	0.72	400	2.65
Hugot *et al*[17]	0.7	724	4.83
	0.7	665	4.43
Szewczyk[18]	6.7	534	2.02

flux q''. The observations have been catalogued in terms of Pr and the number G^* defined[11] as:

$$G^* = 5^{4/5}\left(\frac{g\beta q'' H^4}{k\nu^2}\right)^{1/5} \tag{49}$$

In order to obtain the relationship between N_B and G^*, we make the observation that for $Pr > 1$ fluids the thermal boundary layer thickness and vertical velocity scale[23] as:

$$\delta_T \sim H\left(\frac{g\beta q'' H^4}{k\nu\alpha}\right)^{-1/5} \tag{50}$$

$$u \sim \frac{\alpha H}{\delta_T^2} \tag{51}$$

Substituting $D \sim \delta_T Pr^{1/2}$ and $U \sim u$ into Eq (29) yields:

$$N_B \sim \frac{G^*}{210 Pr^{3/10}} \tag{52}$$

The N_B values corresponding to the experimental observations are listed in the last column of Table 2. Once again, the measured N_B number is of order one, in agreement with the theoretical criterion.

Fig 4 summarizes Tables 1 and 2. The experimental observations on transition fall consistently in the $O(N_B) = 1$ domain in the Prandtl number range 0.7–11.4.

Table 2 Experimental observations on beginning of transition along a wall with constant heat flux

	Pr	G	N_B
Mahajan and Gebhart[11]	0.71	388–620	2.05–3.27
	0.71	400–650	2.11–3.43
Jaluria and Gebhart[19]	6.7	504–802	1.36–2.16
	6.7	563–802	1.52–2.16
Godaux and Gebhart[20]	6.7	528–979	1.42–2.63
Vliet and Liu[21]	6.2	855	2.36
	6.4	955	2.61
	6.4	900	2.46
	5.05	960	2.81
Lock and Trotter[22]	11.0	293	0.68
	11.4	368	0.84

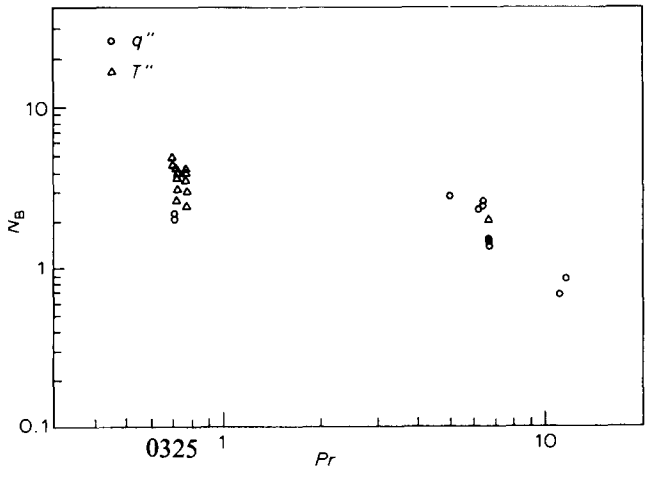

Fig 4 Variation of time ratio N_B with Pr

Transition in enclosures heated from the side

In the preceding section we saw that the experimental observations on transition accumulated over the past three decades support the idea that the fluctuation (waving) time t_{min} matches the time of viscous diffusion across the wall jet. Now, by focusing on enclosures heated from the side, we have the opportunity to actually see the incipient waviness of the two wall jets during transition. The visualisation of the wall jet wavelength λ is made possible by the slow motion of the 'core'[24], ie the motion of the cavity fluid sandwiched between the two fast-moving wall jets. It has been discovered experimentally[25] that in a characteristic Rayleigh number range the core fluid engages in a cellular motion of the type shown schematically in Fig 5. A large number of experimental and numerical studies have confirmed this phenomenon, especially the fact that the number of core cells increases as the Rayleigh number increases. Table 3 shows a representative sample of experimental and numerical observations.

In view of the theoretical discussion presented earlier, it is reasonable to regard the cellular structure of the slow-moving core as the reflection (the fingerprint) of the waviness acquired by the wall jets during transition. Thus, the cell-to-cell distance visible in

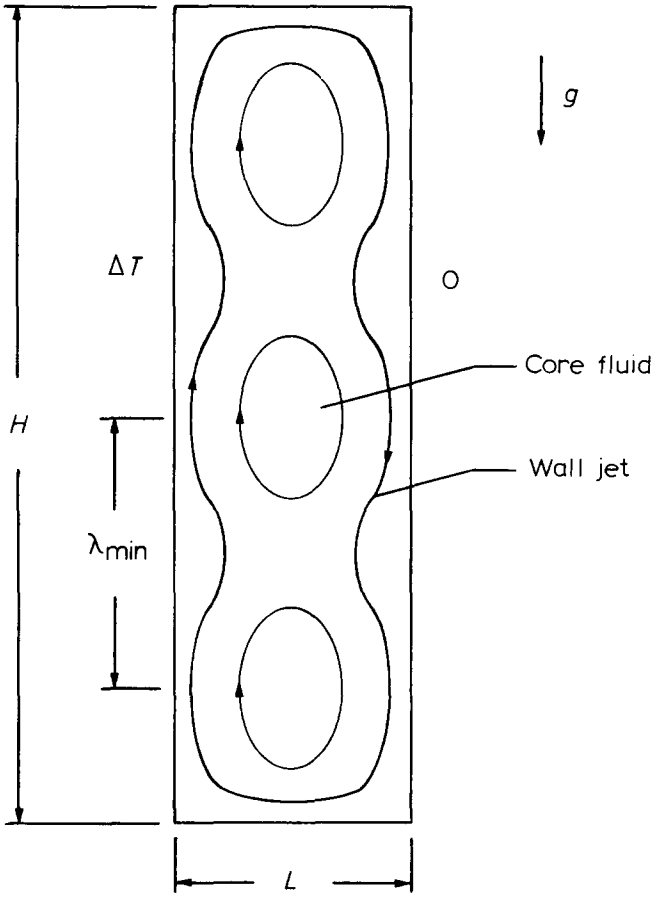

Fig 5 Representation of buoyancy induced flow in a cavity of large aspect ratio with one wall heated, the other cooled, and the top and bottom insulated

published photographs[25-29] can be interpreted as the wavelength λ_{min} of the wall jet. The distance we measured from each photograph is listed as $(H/\lambda_{min})_{experimental}$ in Table 3.

Fig 6 shows the relationship between the measured H/λ_{min} and Ra_H. The wavelength λ_{min} decreases as the Rayleigh number increases. However, the data supplied by an individual experiment (at constant Pr) show very clearly the existence of a proportionality of the type:

$$\frac{H}{\lambda_{min}} \sim Ra_H^{1/4} \tag{53}$$

Theoretically, such a proportionality is to be expected because $\lambda_{min} \sim D$ and $D \sim H\,Ra^{-1/4}$ (Eqs 41 and 46). Thus the core flow data of Table 3 and Fig 6 reconfirm the theoretical result that at transition the jet wavelength always scales with the jet thickness.

The theoretical scale of H/λ_{min} can be calculated by writing $\lambda_{min} = 1.833D$, and by using Eqs (41, 46) to evaluate the scale of D. Thus we obtain:

$$\left(\frac{H}{\lambda_{min}}\right)_{theory} \sim \frac{Ra_H^{1/4}}{1.833\,Pr^{1/2}} \tag{54}$$

for $Pr \gg 1$, and:

$$\left(\frac{H}{\lambda_{min}}\right)_{theory} \sim \frac{Ra_H^{1/4}\,Pr^{1/4}}{1.833} \tag{55}$$

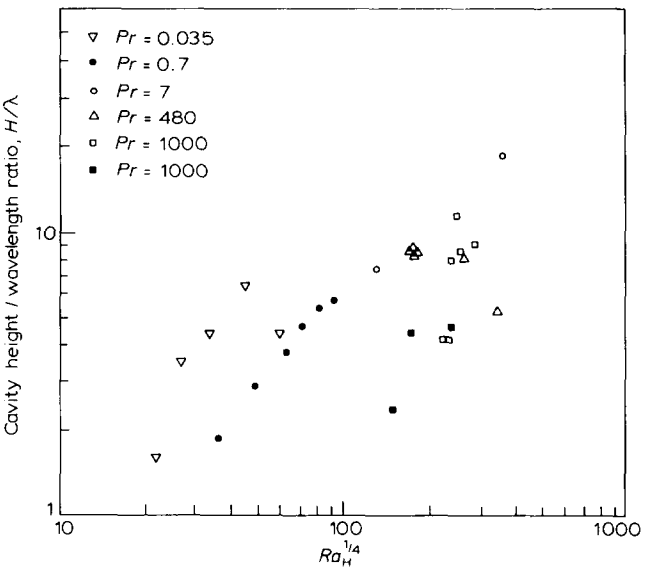

Fig 6 Variation of H/λ *with* $Ra_H^{1/4}$

for $Pr \ll 1$. The theoretical order of magnitude of H/λ_{min} is also listed in Table 3. Finally, the ratio $(\lambda_{min})_{exp}/(\lambda_{min})_{theory}$ was calculated and plotted in Fig 7. It is clear that the measured cell-to-cell distance, $(\lambda_{min})_{exp}$, has the same scale as the theoretical λ_{min}

Table 3 Experimental and numerical observations on transition to turbulence in enclosures heated from the side

	Pr	Ra_H	H/L	H/λ_{min} Experimental	H/λ_{min} Theoretical
Jones[26]	0.035	2.5×10^5	10	1.61	5.28
	0.035	5.0×10^5	10	3.49	6.27
	0.035	1.0×10^6	10	4.36	7.46
	0.035	4.0×10^6	20	6.45	10.55
	0.035	1.1×10^7	20	4.42	10.59
Lee and Korpela[27]	0.7	1.8×10^6	5.0	1.87	18.28
	0.7	6.0×10^6	7.5	2.81	24.7
	0.7	1.4×10^7	10.0	3.73	30.52
	0.7	2.8×10^7	12.5	4.65	36.30
	0.7	4.8×10^7	15.0	5.37	41.54
	0.7	7.6×10^7	17.5	5.67	46.59
	0.7	1.1×10^8	20.0	7.46	51.10
Elder[25]	7	1.7×10^{10}	9.1	18.90	74.46
Seki *et al*[28]	480	9.5×10^8	30	8.60	4.37
	480	9.5×10^8	6	8.80	4.37
	480	1.0×10^9	15	8.39	4.43
	480	5.0×10^9	15	8.40	6.62
	480	1.5×10^{10}	15	5.40	8.71
Elder[25]	1000	2.5×10^9	19	4.17	3.86
	1000	2.7×10^9	19	4.17	3.07
	1000	3.4×10^9	19	7.98	4.17
	1000	4.0×10^9	19	11.54	4.34
	1000	4.7×10^9	19	8.57	4.52
	1000	7.2×10^9	19	9.10	5.03
de Vahl Davis and Mallinson[29]	1000	5.0×10^8	10	2.32	2.58
	1000	9.5×10^8	10	4.36	3.03
	1000	3.3×10^9	10	4.55	4.13

scale predicted by Eqs (54 and 55). The best agreement between $(\lambda_{min})_{exp}$ and $(\lambda_{min})_{theory}$ occurs at extreme Prandtl numbers ($Pr = 0.035$ and $Pr \geq 480$): This is a direct consequence of the fact that scales (54 and 55) are valid strictly in the limits $Pr \to \infty$ and $Pr \to 0$, respectively. The in-between experimental results ($Pr = 0.7$) are least accurately represented by either Eq (54) or Eq (55); nevertheless, the ratio $(\lambda_{min})_{exp}/(\lambda_{min})_{theory}$ for $Pr = 0.7$ is practically independent of Ra_H, stressing the earlier conclusion that λ_{min} always scales with the thickness of the wall jet.

It is worth noting that the $(\lambda_{min}/H) \sim Ra_H^{-1/4}$ scaling law recommended by the time scale criterion (28) is consistent not only with the 27 experiments reviewed in Table 3 and Figs 6 and 7, but also with theoretical results known already from the hydrodynamic stability analysis of the vertical enclosure flow. Attention is drawn to Bergholz's comprehensive study of the flow stability in a vertical slot[30]. As 'base flow' for the stability analysis, Bergholz considered a counterflow velocity profile independent of altitude, as would be the case only in an infinitely tall cavity[31]. He then accounted for the finiteness of the cavity aspect ratio H/L by postulating the existence of a constant vertical temperature gradient through the slot, S[K/m]: note that in the vertical boundary layer regime, the thermal stratification S is of order $\Delta T/H$, where ΔT is the temperature difference in the horizontal direction (Fig 5). By increasing the dimensionless stratification parameter $\gamma = (\frac{1}{4}S(L/\Delta T)Ra_L)^{1/4}$, Bergholz was able to make the base flow more jet-like, that is more like the vertical wall jets of Figs 1 and 3, which are known to prevail in vertical enclosures in the boundary layer regime[24,25].

In Fig 7 of his study, Bergholz reported the critical wavenumber $\alpha_c = 2\pi L/\lambda_c$ versus the stability parameter γ and the Prandtl number. One very interesting aspect of Fig 7 is that in the boundary layer limit ($\gamma \gg 1$) and in the high Prandtl number limit $Pr \to \infty$, the wavenumber of travelling modes is proportional to γ:

$$\alpha_c \sim \gamma, \tag{56}$$

the proportionality constant being a number of order O(1) (in the same limits, the wavenumbers of the stationary modes are, numerically, not much different than those of the travelling modes, however, they do not appear to follow the line represented by Eq (56)).

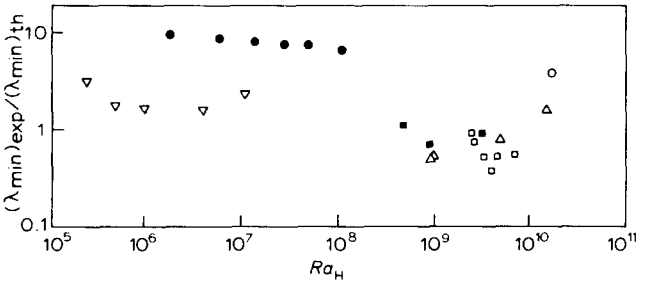

Fig 7 Experimental/theoretical inviscid wavelength ratio as a function of Ra *and* Pr *(*Pr *notation as for Fig 6)*

Noting the L-based definitions of both α_c and γ employed by Bergholz[30], it is easy to prove that the $\alpha_c \sim \gamma$ scaling illustrated by Bergholz is actually:

$$\frac{H}{\lambda_c} \sim Ra_H^{1/4} \tag{57}$$

This scaling, predicted by the conventional stability theory[30] is the same as the scaling law (53) produced by a much more direct argument above.

The agreement between the present approach and conventional stability theory is illustrated further by the fact that α_c reaches asymptotically a O(1) constant as γ approaches zero. This is shown by Fig 7 in Bergholz[30], but is also predicted by the $\lambda_{min} \sim D$ scaling on which the present argument is based. Note that as γ decreases towards zero, the vertical jet thickness increases and so does the wavelength (Eq (56)); but this process cannot continue beyond the point where the jet thickness becomes of order L because, regardless of how small γ is, the slot of width L must house two jets in counterflow. According to the $\lambda_{min} \sim D$ scaling, both D and λ_{min} must be of order L when $\gamma < O(1)$: this also means '$\alpha_c \to O(1)$ constant as $\gamma \to 0$', which is precisely the behaviour unveiled by classical stability analysis (travelling as well as stationary modes, Fig 7 of Ref 30).

Although the compatibility between the results of conventional stability theory and the scaling results based on the argument given earlier is relevant and interesting, one should not expect one theory to 'reproduce' the results of a different theory. Unlike stability theory, which is a mathematically precise approach, the present theoretical argument is approximate and based on the comparison of scales. This is why the success of the present argument should be measured in terms of its ability to predict the trends and orders of magnitude revealed by the many independent experiments collected in Tables 1–3.

Concluding remarks

The published observations on transition to turbulence in natural convection were reviewed in order to test the validity of the time scale criterion (Fig 2) for transition $O(N_B) = 1$ or $O(Re) = 10^2$ formulated. It was found that laboratory observations and numerical simulations support the theoretical viewpoint that:

1. At transition, the wall jet exhibits a unique wavelength which always scales with the thickness of the jet.
2. Transition is marked by the equivalence of two time scales, both properties of the jet region of the flow, the minimum fluctuation period (t_{min}) and the time of viscous diffusion normal to the jet (t_v).

The empirical evidence on natural convection along vertical heated walls suggests that:

3. Transition along an isothermal wall is correctly anticipated by the criterion $O(N_B) = 1$, where N_B is given by Eq (48).
4. Transition along a vertical wall with uniform heat flux is correctly anticipated by the criterion $O(N_B) = 1$, where N_B is given by Eq (52).

5. The cellular flow exhibited by the core fluid in an enclosure is a reflection of the waviness of the two wall jets during transition. The cell size, or the wall jet wavelength, are correctly described by the scales shown in Eqs (54) and (55).

Finally, the theoretical argument leading to the $O(N_B) = 1$ criterion provides a theoretical basis for the empirical notion that the transition Reynolds number is a flow constant considerably greater than unity.

Acknowledgement

This research was sponsored by the US Office of Naval Research.

References

1. **Tani I.** *Annual Review of Fluid Mechanics, 1969,* **1**, *169–196*
2. **Reshotko E.** Boundary-layer stability and transition. *Annual Review of Fluid Mechanics, 1976,* **8**, *311–349*
3. **Gebhart B.** Natural convection flow, instability and transition. *J. Heat Transfer, 1969,* **91**, *293–309*
4. **Lamb H.** *'Hydrodynamics', Dover, New York (1945), 670–671*
5. **Lord Rayleigh** On the stability, or instability, of certain fluid motions. *Proceedings of the London Mathematical Society, Vol XI, 57–70, 1880*
6. **Bejan A.** Analytical prediction of turbulent heat transfer parameters, *Report CUMER 83-4, Dec 1983, Dept. of Mechanical Eng., University of Colorado, Boulder*
7. **Schlichting H.** *'Boundary Layer Theory', 4th ed., McGraw-Hill, New York, 1960, 72*
8. **Bejan A.** On the buckling property of inviscid jets and the origin of turbulence. *Letters in Heat and Mass Transfer, Vol. 8, 181–194, 1981*
9. **Patterson J. and Imberger J.** Unsteady natural convection in a rectangular cavity. *J. Fluid Mechanics, 1980,* **100**, *65–86*
10. **Gebhart B.** *'Heat Transfer', 2nd ed., McGraw-Hill, New York, 1971, 331*
11. **Mahajan R. L. and Gebhart B.** An experimental determination of transition limits in a vertical natural convection flow adjacent to a surface. *J. Fluid Mechanics, 1979,* **91**, *131–154*
12. **Warner C. and Arpaci V. S.** An experimental investigation of turbulent natural convection in air at low pressure along a vertical heated plate. *Int. J. Heat & Mass Transfer, 1968,* **11**, 397–406
13. **Colak-Antic P.** Hitzdraht messungen des laminar-turbulenten Umschlagas bei freier Konvektion. *Jahrbuch der WGLR, 1964, 1972–1976*
14. **Cheesewright R.** Turbulent natural convection from a vertical plane surface. *J. Heat Transfer, 1968,* **90**, *1–8*
15. **Regnier G. M. and Kaplan C.** Visualization of natural convection on a plane wall and in a vertical gap by differential interferometry. Transitional and turbulent regimes. *Proc. 1963 Heat Transfer Fluid Mech. Inst., Stanford University Press, 94–110, 1963*
16. **Eckert E. R. G. and Soehngen E.** Interferometric studies on the stability and transition to turbulence of a free-convection boundary layer. *Proc. Gen. Disc. Heat Transfer, London, 321–323, 1951*
17. **Hugot, G., Jannot M. and Pirovano A.** *Compte-redu de Fin de Contrat DGST no. 69-01-773, 1971*
18. **Szewczyk A. A.** Stability and transition of the free convection layer along a vertical flat plate. *Int. J. Heat & Mass Transfer, 1962,* **5**, *903–914*
19. **Jaluria Y. and Gebhart B.** On transition mechanisms in vertical natural convection flow, *J. Fluid Mechanics, 1974,* **66**, *309–337*
20. **Godaux R. and Gebhart B.** An experimental study of the transition of natural convection flow adjacent to a vertical surface. *Int. J. Heat & Mass Transfer, 1974,* **17**, *93–107*
21. **Vliet G. C. and Liu C. K.** An experimental study of turbulent natural convection boundary layers. *J. Heat Transfer, 1969,* **91**, 517–531
22. **Lock G. S. and Trotter F. J. de B.** Observations on the structure of a turbulent free convection boundary layer. *Int. J. Heat & Mass Transfer, 1968,* **11**, *1225–1232*
23. **Sparrow E. M.** Laminar free convection on a vertical plate with prescribed nonuniform wall heat flux or prescribed nonuniform wall temperature. *NACA TN3508, July 1955, 18*
24. **Gill A. E.** The boundary layer regime for convection in a rectangular cavity. *J. Fluid Mechanics, 1966,* **26**, *515–536*
25. **Elder J. W.** Laminar convection in a vertical slot. *J. Fluid Mechanics, 1965,* **23**, 77–98
26. **Jones I. P.** *Numerical Predictions from the IOTA2 Code for Natural Convection in Vertical Cavities, paper presented at the Winter Annual Meeting of the ASME, Nov. 1982, Phoenix, Arizona*
27. **Lee Y. and Korpela S. A.** Multicellular natural convection in a vertical slot. *J. Fluid Mechanics, 1983,* **126**, *91–121*
28. **Seki N., Fukusako S. and Inaba H.** Visual observations of natural convective flow in a narrow vertical cavity. *J. Fluid Mechanics, 1978,* **84**, *Part 4, 695–704*
29. **de Vahl Davis G. and Mallinson G. D.** A note on natural convection in a vertical slot. *J. Fluid Mechanics, 1975,* **72**, *Part 1, 87–93*
30. **Bergholz R. F.** Instability of steady natural convection in a vertical fluid layer. *J. Fluid Mechanics, 1978,* **84**, *743–768*
31. **Batchelor G. K.** Heat transfer by free convection across a closed cavity between vertical boundaries at different temperatures. *Quarterly of Applied Mathematics, 1954,* **12**, *209–233*